A microwave coaxial sensor for non-destructive detection and analysis of cracked teeth

Zhen Li[1*], Jinjin Qi[2], Zhaozong Meng[3], Ping Wang[1], Constantinos Soutis[4], and Andrew Gibson[5]

[1]College of Automation Engineering, Nanjing University of Aeronautics and Astronautics, Nanjing, 211106, China

[2]Department of Endodontics, Kangjie Dental Clinic, Suzhou, 215008, China

[3]School of Mechanical Engineering, Hebei University of Technology, Tianjin, 300130, China

[4]Department of Materials, The University of Manchester, Manchester, M13 9PL, UK

[5]Faculty of Science and Engineering, Manchester Metropolitan University, Manchester, M1 5GD, UK

[*]Corresponding author: zhenli@nuaa.edu.cn

Abstract: A new approach for the detection of cracks in a tooth is presented using a microwave coaxial sensor. In the test, the probe tip is in close contact with the tooth surface, and the fringe electromagnetic fields out of the probe aperture interact with the tooth material. The presence of any crack affects the effective permittivity, causing changes in the signal energy received. Cracks in two representative teeth are evaluated, and they cannot be readily identified in X-ray images. Low signal power was applied during the scan, and no heating effect was produced. From the scanning of the positions right on and away from the cracks, significant differences are seen in the magnitude and phase of the reflection coefficient. By comparison, it is found that good performance can be achieved using the phase at a high frequency. The probe is also used for permittivity determination. From the measurement of standard liquids, high accuracy is achieved. The permittivity of the crown is computed using the error correction technique, and the data are used in further analytical modelling. In the analysis, by varying the thickness of the dielectric layer, the phase greatly changes when the thickness is below the aperture diameter. Thus, the characteristic of the limited signal penetration is revealed, enabling local inspection and accurate identification. With a simplified geometric model, it is shown that the air gap between the probe tip and the tooth surface does not contribute much to the whole sensing volume. In addition, from the numerical simulation, there is close correlation between the extent of the crack and the phase value, suggesting the potential for quantitative characterisation. The methodology proposed here could provide an alternative solution to efficient non-destructive detection of cracked teeth.

Keywords: cracked teeth; non-destructive detection; microwave technique; coaxial probe; permittivity

1 Introduction

A cracked tooth can be caused by aging, grinding, chewing/biting hard foods or large fillings that reduce the integrity of the tooth. It is a common condition that leads to tooth loss [1]. The crack types include craze lines, fractured cusp, cracks that extend into the gum line, split tooth and vertical root fracture. In the early stages, crack lines in the enamel may not be visible and produce any symptoms. If remained undetected, the crack may extend to dentine or even the pulp cavity, inducing inflammation of the pulp. Thus, timely diagnosis of tooth cracks is of vital importance.

A number of methods have been employed for the detection, such as application of a blue dye, microscopic examination with a magnifying glass, transillumination, cone-beam computed tomographic (CBCT) imaging [2] and magnetic resonance imaging (MRI) [3]. The accuracy of the first three methods is highly dependent on the experience of endodontists. Transillumination is more used for identifying cracks near the root end. However, clinically, most of the cracks exist in the crown of the tooth, and the severity of the crack affects the treatment plan. Small cracks cannot be readily located by CBCT imaging, and the risk of ionising radiation should not be neglected. Better image quality can be provided by MRI, where large and expensive equipment is involved. Therefore, each method has limitations and field of application, and there is a continued search for other kinds of approaches for efficient detection.

In recent years, microwave testing as one of the emerging non-destructive testing (NDT) techniques has received increased interest, due to the advantages of simple setup, one-sided scanning, low signal power and no ionising hazards [4], [5]. For general non-magnetic materials like teeth, the electric permittivity (also called dielectric properties) $\varepsilon=\varepsilon_0\varepsilon_r=\varepsilon_0(\varepsilon_r' - j\,\varepsilon_r'')$, one of the intrinsic physical properties, is associated with the interaction between the material and the incident electromagnetic waves. ε_0 is the permittivity of free space, and ε_r is the relative permittivity. The real part ε_r' of ε_r characterises the energy storage capability, while the imaginary part ε_r'' is related to energy loss. The microwave methods have been widely used for the evaluation of composite structures [6]–[8], coating thickness measurement [9], food analysis [10]–[14], multiphase flows [15] and security check [16], [17]. However, very little research has been carried out in the field of dentistry. Hoshi et al. [18] investigated the effect of dental caries on signal transmission. In the experiment, a tooth with visible caries was placed between two rectangular waveguides, and the caries caused more energy loss compared with a healthy tooth. It is noted that the transmission arrangement is not practical for medical diagnosis. For the purpose of biodosimetry, Meaney et al. [19] compared the permittivity of tooth enamel and dental resin samples and noticed that they could be readily distinguished.

In this work, a microwave coaxial probe with a small aperture is applied for the non-destructive detection of cracked teeth. The working principle of the near-field method is introduced first. Then, two representative cracked teeth are scanned, and the variations of the magnitude and phase of the reflection coefficient are assessed at varied frequencies. Using analytical modelling, the penetration of the microwave signals in the tooth is thoroughly studied. In addition, the relationship between the crack size and the detection sensitivity is also numerically discussed.

2 Materials and methods

2.1 Materials

The two cracked teeth examined were extracted from patients in Kangjie Dental Clinic, Suzhou, China. The reasons for the extraction were irrelevant to this study, and all the patients gave consent to the use of the teeth. The teeth were stored in hydrogen peroxide before the experiments. The photographs and X-ray images of the two teeth are presented in Figure 1, where red arrows denote the location and path of the cracks. Tooth A was extracted for the occurrence of splitting. However, the two cracks (i.e., Cracks 1 and 2) are barely visible when the two split parts are held together. Tooth B was extracted due to gum infection. Its crown is covered by an artificial dental crown, and the crack extends from the crown to the root end. X-ray scanning was performed with IntraOs 70 X-Ray Equipment (Blue X Imaging S.R.L Co.Ltd., Assago, Italy), and in the images produced three cracks cannot be identified.

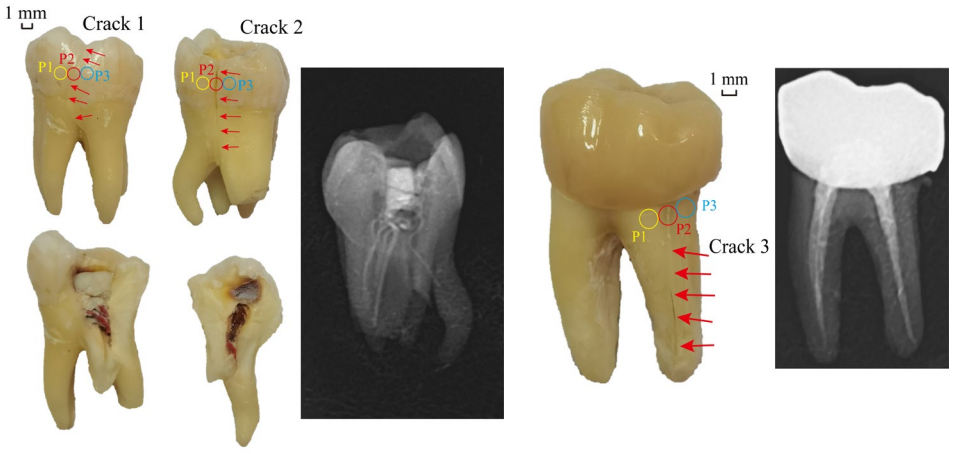

(a) (b)

Figure 1 Photographs and X-ray images of the two cracked teeth used in the study: (a) Tooth A; (b) Tooth B

In Figure 1, Circles P1, P2 and P3 around each crack show the positions where the coaxial probe was placed for scanning. P2 was right on top of the crack. P1 and P3 were on the left and right sides of P2, respectively. The distance between the centres of P1/P3 and P2 (i.e., the diameter of the probe) is significantly larger than the crack size. As the crown is more accessible in practice, for Cracks 1 and

2, the centre of the crack in the crown was chosen. For Crack 3, the top of the crack right below the artificial crown was selected.

Other than the crack detection, the probe was also used for tooth permittivity measurement. Distilled water and ethanol (≥99.8% purity) (Sinopharm Chemical Reagent Co., Ltd, Shanghai, China) were used in the calibration. Two ethanol-water mixtures with mole fractions of ethanol (x_e) of 0.8 and 0.9 were prepared for the verification of the sensor system.

2.2 Microwave sensor and experimental setup

The microwave probe was made with a 30 mm long semi-rigid coaxial cable (Taoglas, Enniscorthy, Ireland), and its maximum operating frequency is 40 GHz. One end of the cable was polished flat, while the other end was terminated with a female Sub-Miniature version A (SMA) connector. The overall cost was around US$12. The experimental setup is schematically illustrated in Figure 2. A tooth was placed on the platform of a laboratory scissor jack. Good contact was made between the probe tip and the region of interest. Some tissue paper was placed below the tooth for better positioning and adjustment. The microwave signal was generated and retrieved with a FieldFox N9951A portable network analyser (Keysight Technologies, Penang, Malaysia). The data of the reflection coefficients (S_{11}) were sent to a personal computer with a LAN cable. A frequency range of 1-40 GHz was used with an intermediate bandwidth (IFBW) of 1 kHz and signal power of -15 dBm (i.e., 0.032 mW). Due to the low signal power used, little heat was generated.

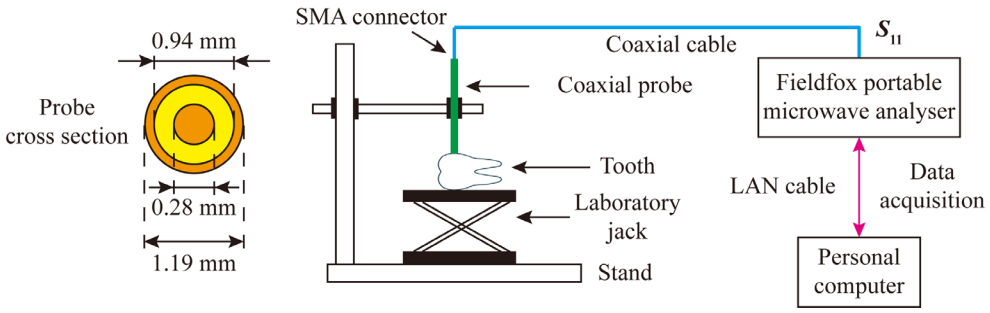

Figure 2 Schematic diagram of the experimental setup for the detection of cracked teeth with a microwave coaxial probe

2.3 Detection principle

In the detection, the evanescent waves near the probe tip interact with the surface and subsurface of the tooth. As presented in Figure 3, an idealised model describing the radiation into an infinite half-space of a dielectric is adopted here, where the tooth is assumed reasonably larger than the probe aperture. The normalised admittance at the probe tip y can be expressed as [20]

$$y = \frac{\varepsilon_r}{\sqrt{\varepsilon_{rc}}\ln(b/a)}\int_0^\infty \frac{\left[J_0(k_0\zeta b) - J_0(k_0\zeta a)\right]^2}{\zeta\sqrt{\varepsilon_r - \zeta^2}}d\zeta \quad (1)$$

where ε_{rc} is the relative permittivity of the dielectric (i.e., Teflon) in the coaxial probe, approximately 2.1 [21]. a is the radius of the inner conductor, while b is the inner radius of the outer conductor. For the probe used, the values of a and b are given in Figure 2. The small probe aperture contributes to fine resolution. J_0 is the zero-order Bessel function of first kind. $k_0=\omega/c$ is the free-space wavenumber. $\omega=2\pi f$ is the angular frequency, and f is the frequency in Hz. c is the speed of light in free space.

The complex reflection coefficient Γ at the probe tip (i.e., ratio of the reflected wave to the incident wave of the electric field strength) can be computed by

$$\Gamma = \frac{1-y}{1+y} \quad (2)$$

From Equations (1) and (2), it is seen that Γ is strongly related to the permittivity of the tooth. In the presence of a crack corresponding to relative permittivity of one, the effective permittivity of the sensing volume is decreased, thereby resulting in changes in Γ and enabling the possibility of detection. It should be mentioned that Γ is slightly different from the S_{11} data, as the reference plane for S_{11} is at the port in the analyser. However, they have larger differences in the phase rather than the magnitude, since the characteristic impedance of the cable is close to that of the coaxial probe. Hence, the effectiveness of using S_{11} in the experiment for indication shall be the same as that of Γ.

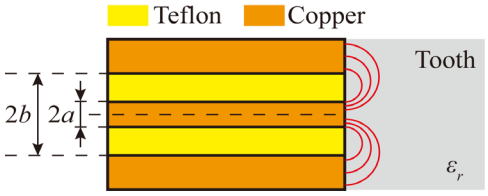

Figure 3 A simplified model for the crack detection of tooth using a microwave coaxial probe

3 Results and Discussion

3.1 Signal responses of the cracks

The magnitude responses at all the nine positions chosen are plotted in Figure 4, where the curves are closely aligned and cannot be readily differentiated. Similar patterns are also found in the phase, so the phase curves are not presented here. Instead, the magnitude and phase data at eight frequencies, from 5 GHz to 40 GHz with an interval of 5 GHz, are evaluated in detail. As shown in Figure 5, for each crack, the magnitude and phase values at the central position are larger than those at the nearby positions. In the scanning, each position was measured three times, and the standard deviations for

the magnitude and phase measurements are around 0.016 dB and 0.41 degree, respectively. The errors are relatively small compared with the mean values, and error bars are not added for better clarity. Further, the signal differences between the central and the other two positions are listed in Table 1. It is indicated that the best performance can be offered at around 35 GHz, the values at which are over ten times larger than those at 5 GHz. Therefore, in terms of the dynamic range provided and measurement errors, the phase parameter is preferred for the crack detection.

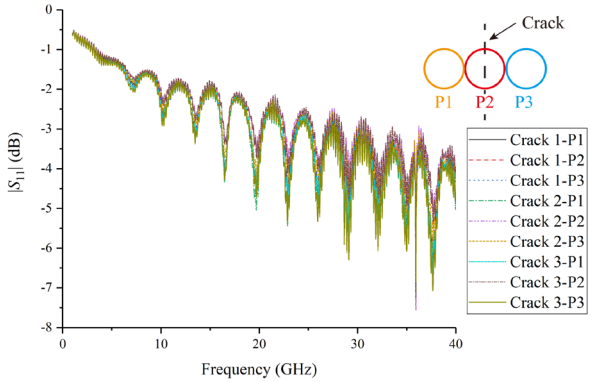

Figure 4 Magnitudes of the reflection coefficients at nine positions of the three cracks

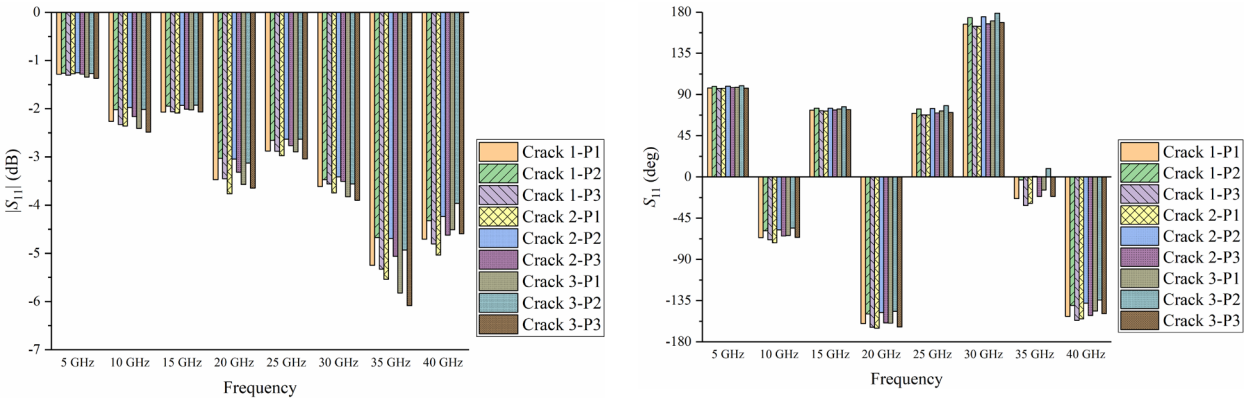

(a) (b)

Figure 5 Responses of the three cracks at eight frequencies: (a) magnitude; (b) phase

Table 1 Mean signal differences between the central and the other two positions for each crack

Frequency	Magnitude (dB)			Phase (degree)		
(GHz)	Crack 1	Crack 2	Crack 3	Crack 1	Crack 2	Crack 3
5	0.034	0.023	0.087	1.85	1.85	2.33
10	0.278	0.285	0.432	8.58	10.34	9.11
15	0.120	0.120	0.117	2.22	2.52	2.65
20	0.436	0.497	0.483	12.53	14.25	14.90
25	0.223	0.239	0.336	5.53	5.98	6.58
30	0.116	0.213	0.301	8.12	9.17	9.40
35	0.619	0.611	1.018	24.04	25.80	26.99
40	0.435	0.593	0.589	14.24	15.31	13.42

3.2 Penetration of the microwave signal in the tooth

First, the permittivity of Tooth A at four arbitrarily chosen positions of the crown was measured. The error correction technique is employed here for the permittivity calculation. The permittivity of the material under test ε_m can be computed by [13]

$$\varepsilon_m = -\frac{\Delta_{m1}\Delta_{32}\varepsilon_3\varepsilon_2 + \Delta_{m2}\Delta_{13}\varepsilon_1\varepsilon_3 + \Delta_{m3}\Delta_{21}\varepsilon_2\varepsilon_1}{\Delta_{m1}\Delta_{32}\varepsilon_1 + \Delta_{m2}\Delta_{13}\varepsilon_2 + \Delta_{m3}\Delta_{21}\varepsilon_3} \tag{3}$$

where ε_1, ε_2 and ε_3 are the relative permittivity of three standards used for calibration. In the present case, Standards 1, 2 and 3 are an open circuit, water and ethanol, respectively. The open circuit is done by leaving the probe open in the air (i.e., ε_1=1). $\Delta_{ij}=\rho_i-\rho_j$, where ρ_1, ρ_2 and ρ_3 are the measured reflection coefficients. ρ_m is the reflection coefficient corresponding to the sample. The reference permittivity data of pure water and ethanol solutions (both pure and diluted ethanol) are taken from References [22] and [23], respectively. The maximum frequency of the ethanol permittivity data is 20 GHz, so a frequency range of 1-20 GHz was set. As seen in Figure 6, for diluted ethanol samples, there is good agreement between the references and the present work. The errors of ε_r' and ε_r'' are well within ±5% over the whole frequency range, confirming high accuracy.

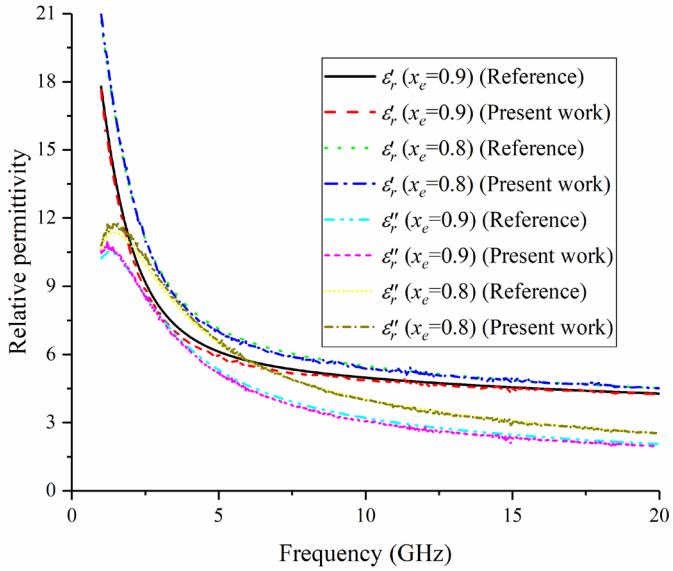

Figure 6 Comparison of the permittivity values of diluted ethanol samples offered by the reference and the present work

For Tooth A, the permittivity at four representative positions of the crown was measured. As presented in Figure 7, the ε_r' and ε_r'' values are relatively stable over the frequency range. Thus, the average value 5.38-*j*0.67 is used in the following analysis.

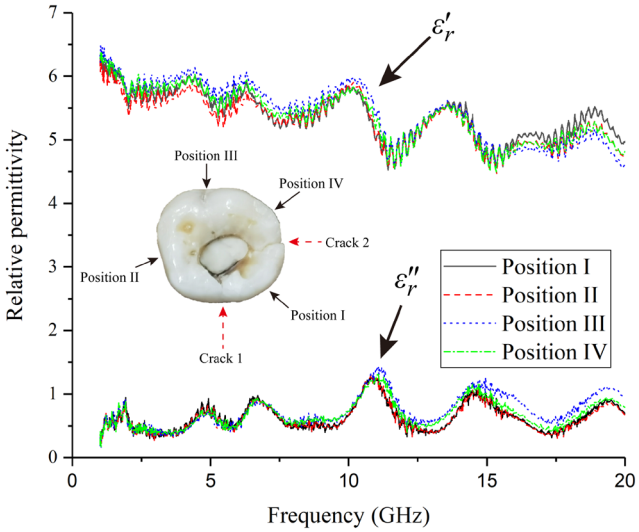

Figure 7 Relative permittivity spectra of the crown of Tooth A at four representative positions

Using the permittivity results, the signal penetration at 35 GHz is evaluated with a variant of the analytical model mentioned [24], where a dielectric sample with a finite thickness (d_t) is backed by free space. As seen in Figure 8, the phase sharply decreases as d_t increases from 0 to 1 mm, while there is little fluctuation at larger d_t values. Hence, the maximum depth that the sensor can detect the dielectric inhomogeneity is around 1 mm, which is comparable to the aperture diameter. The low penetration well demonstrates the distinctive advantage of local sensing of the probe. It is also suggested that the permittivity measured primarily corresponds to the enamel layer.

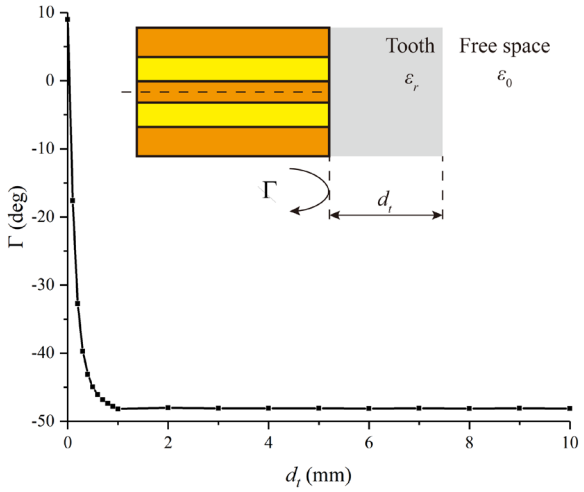

Figure 8 Variation of the phase simulated at varied thicknesses of the dielectric layer

3.3 Crack size effect on the detection performance

First, as shown in Figure 9, a simple geometric model is built to analyse the minute air gap (i.e., the shaded region) between the probe tip and the tooth surface in the real setup. The curvature of the tooth surface is assumed close to that of a sphere with a radius of R (approximately 6.17 mm for Tooth A). The volume that can be sensed by the probe can be determined by

$$V_s = \pi r^2 \delta_s \tag{4}$$

where r is the outer radius of the dielectric in the coaxial probe (i.e., 0.47 mm). δ_s denotes the penetration depth, which is commonly used to describe the extent that an electromagnetic signal is attenuated within a medium. It is the depth where the signal magnitude is reduced to $1/e$ (about 37 %) of its original value [25]

$$\delta_s = \frac{c}{\sqrt{2}\pi f \left\{ \varepsilon_r' \left[\sqrt{1 + \left(\frac{\varepsilon_r''}{\varepsilon_r'} \right)^2} - 1 \right] \right\}^{1/2}} \tag{5}$$

In the present case, the dimension of the tooth along the probe (d) is considerably larger than δ_s. Hence, δ_s is used in the estimation.

The volume of the air gap can be given by

$$V_a = \frac{\pi R^3}{3} \left(-2\sin^2\varphi\cos\varphi + 3\sin^2\varphi + 2\cos\varphi - 2 \right) \tag{6}$$

where the angle φ can be determined by $\sin^{-1}(r/R)$. Therefore, the ratio of the volume of the gap to that of the sensing volume can be evaluated by

$$\xi = \frac{V_a}{V_s} = \frac{R\left[-2\cos\varphi + 3 - \sec\left(\varphi/2\right) \right]}{3\delta_s} \tag{7}$$

By substituting the known values of r, R and δ_s into Equation (7), it is calculated that ξ is well below 1%. Therefore, it is reasonable to ignore the air gap in studying the crack, where the infinite half-space model is used. The structure of a real crack is complicated, so here the crack and tooth are treated as one material, the effective permittivity of which ε_{eff} is estimated by the law of mixture.

$$\varepsilon_{\text{eff}} = \nu_c + (1 - \nu_c)\varepsilon_r \tag{8}$$

where ν_c is the volume fraction of the crack in the sensing volume. ε_{eff} decreases with increasing crack size. In the simulation, the built-in Matlab® function *integral* is used for fast calculation of the integration in Equation (1). The relationship between the phase of Γ at 35 GHz and ν_c is shown in Figure 10. Here only the data at very low ν_c values are given to satisfy the condition of Equation (8) for a macroscopic crack. The phase change increases with increasing ν_c, and a linear relationship is revealed with a high coefficient of determination. In the fitted equation the intercept is not zero, but it is much smaller than the dynamic range of the phase shift. Thus, it is indicated that the phase could help characterise the extent of the crack.

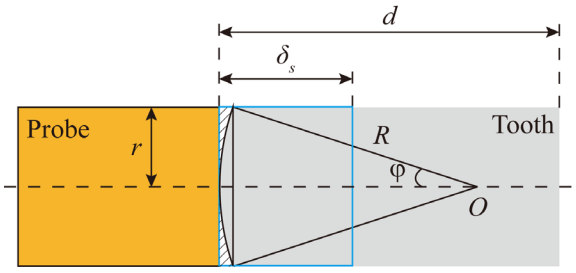

Figure 9 A geometric model considering the gap between the probe tip and curved tooth surface

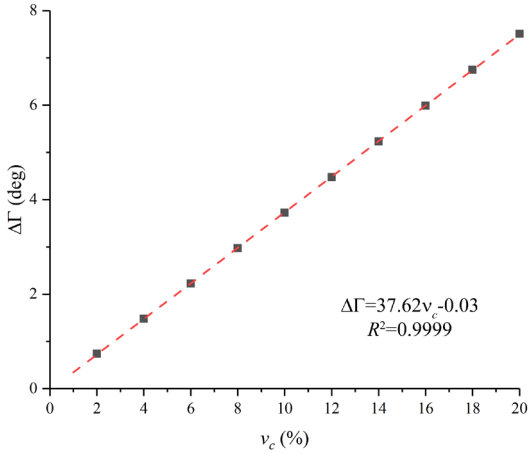

Figure 10 Changes of the phase simulated at different volume fractions of the crack with respect to the case with no crack

4 Concluding remarks

The microwave coaxial probe has been successfully applied for the evaluation of cracked teeth. From the scanning, it has been shown that the presence of the crack can be well detected at 35 GHz using the phase of the reflection coefficient. A phase threshold can be defined to better accommodate practical applications. From the analytical modelling, the penetration is shown limited with the depth close to the probe aperture size, which is advantageous for the localised interrogation. In the study of the crack size on the performance, a linear relationship has been established between the extent of the crack and the magnitude of the signal received, facilitating quantitative evaluation. For future work, the applicability of the method presented will be explored in a clinical setting. A smaller probe and bespoke design of a low-cost microwave source will be made.

Acknowledgements

This work was financially supported by the Natural Science Foundation of Jiangsu Province (Grant No. BK20200427), the Shuangchuang Project of Jiangsu Province (Grant No. KFR20020) and the

National Natural Science Foundation of China (Grant No. 52105552). The first author gratefully acknowledges Dr.Zhijun Chen for many useful discussions. Special thanks to Dr.Fei Fei and Dr.Changcheng Wu for assistance in the experiments.

References

[1] E. B. LUBISICH, T. J. HILTON, and J. FERRACANE, “Cracked Teeth: A Review of the Literature,” *J. Esthet. Restor. Dent.*, vol. 22, no. 3, pp. 158–167, Jun. 2010.

[2] M. Yuan *et al.*, “Using Meglumine Diatrizoate to improve the accuracy of diagnosis of cracked teeth on Cone-beam CT images,” *Int. Endod. J.*, vol. 53, no. 5, pp. 709–714, May 2020.

[3] T. J. Schuurmans *et al.*, “Accuracy and Reliability of Root Crack and Fracture Detection in Teeth Using Magnetic Resonance Imaging,” *J. Endod.*, vol. 45, no. 6, pp. 750-755.e2, Jun. 2019.

[4] K. Brinker, M. Dvorsky, M. T. Al Qaseer, and R. Zoughi, “Review of advances in microwave and millimetre-wave NDT&E: principles and applications,” *Philos. Trans. R. Soc. A Math. Phys. Eng. Sci.*, vol. 378, no. 2182, p. 20190585, Oct. 2020.

[5] Z. Li, P. Wang, A. Haigh, C. Soutis, and A. Gibson, “Review of microwave techniques used in the manufacture and fault detection of aircraft composites,” *Aeronaut. J.*, vol. 125, no. 1283, pp. 151–179, Jan. 2021.

[6] Z. Li *et al.*, “Detection of Impact Damage in Carbon Fiber Composites Using an Electromagnetic Sensor,” *Res. Nondestruct. Eval.*, vol. 29, no. 3, pp. 123–142, Jul. 2018.

[7] Z. Li, T. Wang, A. Haigh, Z. Meng, and P. Wang, “Non-contact detection of impact damage in carbon fibre composites using a complementary split-ring resonator sensor,” *J. Electr. Eng.*, vol. 70, no. 6, pp. 489–493, Dec. 2019.

[8] Z. Li, A. Haigh, C. Soutis, A. Gibson, and R. Sloan, “Microwaves Sensor for Wind Turbine Blade Inspection,” *Appl. Compos. Mater.*, vol. 24, no. 2, pp. 495–512, Apr. 2017.

[9] Z. Li, Z. Meng, C. Soutis, A. Haigh, P. Wang, and A. Gibson, “Bimodal Microwave Method for Thickness Estimation of Surface Coatings on Polymer Composites,” *Adv. Eng. Mater.*, p. 2100494, Aug. 2021.

[10] M. E. Sosa-Morales, L. Valerio-Junco, A. López-Malo, and H. S. García, “Dielectric properties of foods: Reported data in the 21st Century and their potential applications,” *LWT - Food Sci. Technol.*, vol. 43, no. 8, pp. 1169–1179, Oct. 2010.

[11] Z. Li, Z. Meng, A. Haigh, P. Wang, and A. Gibson, “Characterisation of water in honey using

a microwave cylindrical cavity resonator sensor," *J. Food Eng.*, vol. 292, p. 110373, Mar. 2021.

[12] Z. Li, A. Haigh, P. Wang, C. Soutis, and A. Gibson, "Characterisation and analysis of alcohol in baijiu with a microwave cavity resonator," *LWT*, vol. 141, p. 110849, Apr. 2021.

[13] Z. Li, A. Haigh, P. Wang, C. Soutis, and A. Gibson, "Dielectric spectroscopy of Baijiu over 2–20 GHz using an open-ended coaxial probe," *J. Food Sci.*, vol. 86, no. 6, pp. 2513–2524, Jun. 2021.

[14] A. A. P. Gibson *et al.*, "An overview of microwave techniques for the efficient measurement of food materials," *Food Manuf. Effic.*, vol. 2, no. 1, pp. 35–43, 2008.

[15] E. Bondet de la Bernardie *et al.*, "Low (10–800 MHz) and high (40 GHz) frequency probes applied to petroleum multiphase flow characterization," *Meas. Sci. Technol.*, vol. 19, no. 5, p. 055602, May 2008.

[16] D. A. Andrews, S. W. Harmer, N. J. Bowring, N. D. Rezgui, and M. J. Southgate, "Active millimeter wave sensor for standoff concealed threat detection," *IEEE Sens. J.*, vol. 13, no. 12, pp. 4948–4954, Dec. 2013.

[17] B. Y. Kapilevich, S. W. Harmer, and N. J. Bowring, *Non-Imaging Microwave and Millimetre-Wave Sensors for Concealed Object Detection*. New York: CRC Press, 2014.

[18] N. Hoshi, Y. Nikawa, K. Kawai, and S. Ebisu, "Application of microwaves and millimeter waves for the characterization of teeth for dental diagnosis and treatment," *IEEE Trans. Microw. Theory Tech.*, vol. 46, no. 6, pp. 834–838, Jun. 1998.

[19] P. Meaney, B. Williams, S. Geimer, A. Flood, and H. Swartz, "A Coaxial Dielectric Probe Technique for Distinguishing Tooth Enamel from Dental Resin," *Adv. Biomed. Eng. Res.*, vol. 3, p. 8, 2015.

[20] S. I. Ganchev, N. Qaddoumi, S. Bakhtiari, and R. Zoughi, "Calibration and Measurement of Dielectric Properties of Finite Thickness Composite Sheets with Open-Ended Coaxial Sensors," *IEEE Trans. Instrum. Meas.*, vol. 44, no. 6, pp. 1023–1029, 1995.

[21] A. R. Von Hippel, *Dielectric materials and applications*, 2nd ed. New York: Artech House, 1995.

[22] P. R. Mason, J. B. Hasted, and L. Moore, "The use of statistical theory in fitting equations to dielectric dispersion data," *Adv. Mol. Relax. Process.*, vol. 6, no. 3, pp. 217–232, Nov. 1974.

[23] P. Petong, R. Pottel, and U. Kaatze, "Water−Ethanol Mixtures at Different Compositions and Temperatures:A Dieletric Relaxation Study," *J. Phys. Chem. A*, vol. 104, no. 32, pp. 7420–7428, Aug. 2000.

[24] L. F. Chen, C. K. Ong, C. P. Neo, V. V. Varadan, and V. K. Varadan, *Microwave Electronics: Measurement and Materials Characterization*. Chichester, UK: John Wiley & Sons, Ltd, 2004.

[25] D. M. Pozar, *Microwave Engineering*, Fourth edi. New York: John Wiley & Sons, 2012.